Diffraction theory of scattering by rotating nuclei

Göran Fäldt
Gustaf Werner Institute, Box 535, S-75121 Uppsala, Sweden

Roy Glauber
Lyman Laboratory of Physics, Harvard University, Cambridge, Massachusetts 02138

(Received 2 August 1989)

We investigate, within the context of diffractive collision theory, the elastic and inelastic scattering of high-energy particles by permanently deformed, axially symmetric nuclei. The nuclear matter density and optical potential are expanded into multipole contributions of order $L=0,2,4,\ldots$. We first consider the dominant multipoles $L=0$ and 2 alone, and determine for this model the scattering amplitude for excitation of a nuclear rotational state with quantum numbers L and M. We then discuss a procedure that permits us to account, by series expansion, for the higher order multipole deformations $L=4,6,\ldots$. The convergence of the method is discussed in connection with explicit numerical examples and various differential cross sections are presented.

I. INTRODUCTION

Considerable effort has been devoted to determining the shapes of nonspherical nuclei. Their electric charge and current distributions have been probed in electron scattering,[1] and their matter distributions in alpha particle[2] and proton[3] scattering. The elastic and inelastic scattering data for these nuclei have customarily been analyzed by means of coupled-channel optical models, a procedure that works well for the first few excited states. The number of angular-momentum-state channels that must be included in these numerical integrations of the Schrödinger equation becomes quite large, however, with increasing transfers of angular momentum. The number of channels included must, in fact, considerably exceed the number of final states observed experimentally since virtual transitions through intermediate states of higher angular momentum must be properly taken into account. Since recent observations of ^{154}Sm and ^{176}Yb have measured excitation of rotational transitions up to $L=8$, that is to say including 25 final rotational states, it seems clear that an alternative approach to the calculation would be desirable.

Nuclear rotational transitions can be accurately treated by means of diffractive collision theory,[4] because they only involve small transfers of energy and have the scattering of high-energy incident hadrons still concentrated near the forward direction. One of the advantages of diffraction theory is that it is not based on any separation of the scattering problem into coupled angular momentum channels. It furnishes closed expressions for the various scattering amplitudes that sum implicitly the contributions of virtual transitions between all intermediate states. The method has already been employed by Abgrall *et al.*[5] to investigate the role of multistep or dispersive contributions to the transition amplitudes. It has also been used by Ginocchio *et al.*[6] in conjunction with the interacting boson model of rotational states. Our aim in the present work is to begin the systematic development of a more general approach to the diffraction theory of rotational transitions.

The nuclei we shall consider are perfect rotators with axially symmetric ground-state densities. In the intrinsic, body-fixed coordinate system, their ground-state density functions can be expanded as

$$\rho(\mathbf{r},\Omega_p)=\sum_{L=0,2,4,\ldots}\rho_L(r)P_L(\cos\Theta)\ , \tag{1.1}$$

where Θ is the colatitude angle of $\mathbf{r}$ relative to the polar, or symmetry axis, which has angular coordinates denoted by Ω_p.

The diffraction theory expresses the scattering amplitude F_{LM} for excitation of the rotational state with quantum numbers L and M in an explicit form as a triple integral. We shall show that two of the required integrations can be carried out, in general, analytically, leaving the third integration, over impact parameters, to be carried out numerically. The general form of these integrals, as we shall see, allows a number of qualitative insights into the shapes of the corresponding differential cross sections. It also gives a simple picture of the distributions of impact parameters over which the various rotational transitions are induced.

After presenting a general discussion of our method in Secs. II and III, we undertake a detailed treatment of the case of pure quadrupole deformation and the scattering amplitudes that result in the two sections that follow. We then turn to the case of higher order multipole deformations and show how they can be treated perturbatively in the next two sections. In the final section we investigate the accuracy of a peripheral approximation introduced by Ginocchio *et al.*[6] to treat the case of strongly absorbing nuclei.

II. GENERAL FORMULATION

The diffraction approximation assumes that the incident particle can penetrate the nucleus by traveling along any of a bundle of straight-line trajectories parallel to the initial momentum. The phase shift function $i\chi(\mathbf{b})$

calculated in this way is closely related to the shadow of the nucleus, cast upon a plane perpendicular to the incident momentum, that is upon the impact plane, or **b** plane. We shall discuss the calculation of the phase shift function in the next section. All we need in order to present the general formulation of the scattering amplitude and cross sections is the awareness that the phase shift function depends on the instantaneous orientation Ω_p of the symmetry axis of the nucleus as well as on the impact vector **b** of the incident nucleon. The nuclear shadow is then described, in effect, by the complex profile function

$$\Gamma(\mathbf{b},\Omega_p)=1-e^{i\chi(\mathbf{b},\Omega_p)} . \tag{2.1}$$

The diffractive approximation we are discussing requires that the wavelength of the incident nucleon be considerably smaller than the nuclear radius. For protons that means in practice incident energies of some hundreds of MeV. The energy separations of the rotational states of deformed nuclei, on the other hand, are usually some tens of keV. These values are small enough to permit the treatment of nuclear rotation as an infinitely slow process relative to the instantaneous passage of the incident nucleons, and to permit the neglect of any actual energy transfer in the calculation of the various rotationally inelastic collision processes. We shall assume then that the deformed nucleus is initially in its rotational ground state, a state in which the symmetry axis Ω_p has the isotropic wave function $Y_0^0(\Omega_p)=(4\pi)^{-1/2}$. Then, if the phase shift function for the incident proton is written as $\chi(b,\Omega_p)$, the amplitude for a scattering process of momentum transfer **q**, in which the axially symmetric nucleus goes to a final rotational state with wave function $Y_L^M(\Omega_p)$, is

$$F_{LM}(\mathbf{q})=\frac{ik}{2\pi}\int d^2b\, e^{i\mathbf{q}\cdot\mathbf{b}}\int Y_L^M(\Omega_p)^\dagger\Gamma(\mathbf{b},\Omega_p)Y_0^0(\Omega_p)d\Omega_p . \tag{2.2}$$

The integration over $d\Omega_p$ in this expression extends over the sphere of orientations of Ω_p. The differential cross section corresponding to this transition is

$$\frac{d\sigma_{LM}}{d\Omega}=|F_{LM}(\mathbf{q})|^2 . \tag{2.3}$$

As we shall see presently, for an axially symmetric nucleus with a density expansion given by Eq. (1.1), this cross section will vanish for all odd values of L.

The diffraction theory furnishes us with particularly simple expressions for the integrated partial cross sections. To integrate the cross section $d\sigma_{LM}/d\Omega$ over angles, for example we multiply it by $1/k^2$ and integrate over d^2q, the two-dimensional element of momentum transfer, lying in the plane perpendicular to the incident momentum. By using the delta-function identity

$$\int d^2q\, e^{i\mathbf{q}\cdot(\mathbf{b}-\mathbf{b}')}=(2\pi)^2\delta^{(2)}(\mathbf{b}-\mathbf{b}') , \tag{2.4}$$

we then find that the integrated cross section σ_{LM} reduces to the single impact parameter integral

$$\sigma_{LM}=\int\frac{d\sigma_{LM}}{d\Omega}d\Omega = \int d^2b\frac{1}{4\pi}\left|\int Y_L^M(\Omega_p)^\dagger\Gamma(\mathbf{b},\Omega_p)d\Omega_p\right|^2 . \tag{2.5}$$

The cross section for elastic scattering, in particular, is given by

$$\sigma_{\rm el}=\sigma_{00}=\int d^2b\left|\int\Gamma(\mathbf{b},\Omega_p)\frac{d\Omega_p}{4\pi}\right|^2 . \tag{2.6}$$

The summed scattering cross section, that is to say the integrated cross section for all elastic and rotationally inelastic scattering processes, is given by

$$\sigma_{\rm sum}=\sum_{L,M}\sigma_{LM} . \tag{2.7}$$

We can easily evaluate this cross section by using the completeness relation for the spherical harmonics

$$\sum_{L,M}Y_L^M(\Omega)^\dagger Y_L^M(\Omega')=\delta(\Omega,\Omega') , \tag{2.8}$$

to find

$$\sigma_{\rm sum}=\int d^2b\int|\Gamma(\mathbf{b},\Omega_p)|^2\frac{d\Omega_p}{4\pi} . \tag{2.9}$$

The part of the inelastic cross section due exclusively to nuclear rotational transitions is evidently

$$\sigma_{\rm sum}-\sigma_{00}=\sum_{L\neq0,M}\sigma_{LM} =\int(\langle|\Gamma(\mathbf{b},\Omega_p)|^2\rangle-|\langle\Gamma(\mathbf{b},\Omega_p)\rangle|^2)d^2b . \tag{2.10}$$

We have used angular brackets in the latter expression to signify mean values taken over all orientations of Ω_p. The quantity integrated over the impact plane is thus the variance of the profile function. It is the fluctuations of the profile function due to the uncertainty in the orientation of the symmetry axis Ω_p, therefore, that are responsible for the inelastic scattering. We shall resolve the fluctuations into their various angular momentum components in the next section.

According to the optical theorem, the total nuclear cross section, which includes all inelastic collision processes, is given by

$$\sigma_{\rm tot}=\frac{4\pi}{k}{\rm Im}F_{00}(0) =2\,{\rm Re}\int d^2b\int\Gamma(\mathbf{b},\Omega_p)\frac{d\Omega_p}{4\pi} =2\int d^2b\int(1-{\rm Re}\,e^{i\chi(\mathbf{b},\Omega_p)})\frac{d\Omega_p}{4\pi} . \tag{2.11}$$

The intrinsic inelastic cross section, which is the part associated with nonrotational transitions is thus, according to Eqs. (2.9) and (2.11),

$$\sigma_{\rm inel}=\sigma_{\rm tot}-\sigma_{\rm sum} =\int d^2b\int(1-|e^{i\chi(\mathbf{b},\Omega_p)}|^2)\frac{d\Omega_p}{4\pi} . \tag{2.12}$$

This expression is, in effect, the absorption cross section for the nucleus averaged over all orientations of the symmetry axis.

III. THE NUCLEAR PHASE SHIFT FUNCTION

In the diffraction approximation the nuclear phase shift function $\chi(\mathbf{b},\Omega_p)$ is determined by the optical thickness of the nucleus at each impact vector $\mathbf{b}$. It is useful therefore to define what we shall call the thickness function

$$t(\mathbf{b},\Omega_p)=\int_{-\infty}^{\infty}\rho(\mathbf{b}+\hat{\kappa}z,\Omega_p)dz \ . \tag{3.1}$$

The vector $\hat{\kappa}$ here is a unit vector in the direction of the incident momentum $\mathbf{k}$ and the integration is carried out over straight-line paths through the instantaneous configuration of the nucleus.

It is useful to separate the dependences of expressions like the thickness function on the coordinates of the incident nucleon and on those of the rotating nucleus. We can make use, for that purpose, of the addition theorem for spherical harmonics to write

$$P_L(\cos\Theta)=\frac{4\pi}{2L+1}\sum_M Y_L^M(\Omega)^\dagger Y_L^M(\Omega_p) \ . \tag{3.2}$$

In this expression $\Omega=(\theta_r,\phi_b)$ represents the angular coordinates of the vector $\mathbf{r}=(\mathbf{b},z)$ in the laboratory system, $\Omega_p=(\theta_p,\phi_p)$ represents the coordinates of the symmetry axis in the same system, and Θ is the angle between $\mathbf{r}$ and the symmetry axis Ω_p.

When Eqs. (3.2) and (1.1) are used to express ρ in the definition (3.1) of the thickness function we find

$$t(\mathbf{b},\Omega_p)=\int\sum_{L,M}\frac{4\pi}{2L+1}\rho_L[(b^2+z^2)^{1/2}] \times Y_L^M(\Omega)^\dagger Y_L^M(\Omega_p)dz \ . \tag{3.3}$$

It is convenient, at this point, to define a set of spherical harmonic components $t_{LM}(b)$ of the thickness function via the relations

$$t_{LM}(b)=\frac{\sqrt{4\pi}}{2L+1}e^{-iM\phi_b}\int_{-\infty}^{\infty}\rho_L[(b^2+z^2)^{1/2}] \times Y_L^M(\theta_r,\phi_b)dz \tag{3.4a}$$

$$t_{LM}(b)=(-1)^M t_{L,-M}(b) \ . \tag{3.4b}$$

We note that the functions $t_{LM}(b)$, defined in this way, depend only on the modulus of the vector $\mathbf{b}$, and not on its azimuthal angle ϕ_b. It follows then that

$$\int_{-\infty}^{\infty}\rho_L[(b^2+z^2)^{1/2}]Y_L^M(\Omega)^\dagger dz =\frac{2L+1}{\sqrt{4\pi}}t_{LM}(b)e^{-iM\phi_b} \ , \tag{3.5}$$

and the expansion (3.3) for the thickness function can be written as

$$t(\mathbf{b},\Omega_p)=\sqrt{4\pi}\sum_{L,M}t_{LM}(b)e^{-iM\phi_b}Y_L^M(\Omega_p) \ . \tag{3.6}$$

We have assumed the nuclear density to be inversion symmetric, $\rho(\mathbf{r})=\rho(-\mathbf{r})$, and so its expansion contains no terms $\rho_L(r)$ for odd L. It follows then that the $t_{LM}(b)$ vanish for all odd values of L. There is another symmetry implicit in the expression (3.1) for the thickness function. Rotating the nucleus by adding π to ϕ_p, or alternatively changing θ_p to $\pi-\theta_p$, will not in general leave the nuclear density unchanged, but it is an invariance transformation of the nuclear shadow. Since the $Y_L^M(\Omega_p)$ are simply multiplied by $(-1)^M$ under this transformation, this symmetry of the expansion (3.6), for example, implies that the $t_{LM}(b)$ also vanish for all odd values of M. We thus have

$$t_{LM}(b)=0 \quad \text{for all odd } L,M \ , \tag{3.7a}$$

and from Eq. (3.4b),

$$t_{L,-M}(b)=t_{L,M}(b) \ . \tag{3.7b}$$

The optical phase shift function $\chi(\mathbf{b},\Omega_p)$ that we seek has approximately the same shape as the thickness function $t(\mathbf{b},\Omega_p)$ that we have been discussing. The proportionality of the two functions is exact in the limit in which the range of the nucleon-nucleon force is much smaller than nuclear dimensions. If the finite size of the force range is to be fully accounted for, however, the phase shift function χ must be regarded as a convolution of the thickness function with the nucleon-nucleon profile function. The latter profile function is defined as[4]

$$\Gamma_n(b)=\frac{1}{2\pi ik}\int e^{-i\mathbf{q}\cdot\mathbf{b}}f(q)d^2q \ , \tag{3.8}$$

where $f(q)$ is the nucleon-nucleon scattering amplitude and the momentum transfer integration is carried out over a plane perpendicular to $\mathbf{k}$.

The convolution integral that defines the optical phase shift function is given by

$$i\chi(\mathbf{b},\Omega_p)=-\int\Gamma_n(|\mathbf{b}-\mathbf{s}|)t(\mathbf{s},\Omega_p)d^2s \ , \tag{3.9}$$

an expression in which the vector $\mathbf{s}$, like $\mathbf{b}$, lies in the impact plane and the integration is extended over that plane. The zero-range approximation for the nucleon-nucleon force corresponds to writing

$$\Gamma_n(\mathbf{b})\simeq\frac{2\pi}{ik}f(0)\delta^{(2)}(\mathbf{b}) \ , \tag{3.10}$$

in which $\delta^{(2)}$ is a two-dimensional delta function. The phase shift function in this approximation is then

$$i\chi(\mathbf{b},\Omega_p)=\frac{2\pi i}{k}f(0)t(\mathbf{b},\Omega_p) =-\tfrac{1}{2}\sigma(1-i\alpha)t(\mathbf{b},\Omega_p) \ , \tag{3.11}$$

where σ is the nucleon-nucleon cross section and $\alpha=\mathrm{Re}f(0)/\mathrm{Im}f(0)$.

To evaluate the more accurate expression (3.9), for the phase shift, it is again essential that we separate, insofar as possible, the spherical harmonic dependences of $\chi(\mathbf{b},\Omega_p)$ on the coordinates of the impact vector $\mathbf{b}$ and those of the symmetry axis Ω_p.

When we substitute the expansion (3.6) for the thickness function in the convolution integral (3.9) we find

$$i\chi(\mathbf{b},\Omega_p)=-\sqrt{4\pi}\sum_{L,M}\int\Gamma_n(|\mathbf{b}-\mathbf{s}|)t_{LM}(s)\times e^{-iM\phi_s}d^2s\,Y_L^M(\Omega_p)\,, \tag{3.12}$$

in which ϕ_r is the azimuthal angle associated with the transverse vector $\mathbf{s}$. We shall find it convenient to express this sum more compactly by defining the functions

$$\chi_{LM}(b)=i\int\Gamma_n(|\mathbf{b}-\mathbf{s}|)e^{iM(\phi_b-\phi_s)}t_{LM}(s)d^2s\,, \tag{3.13}$$

which are invariant under displacements of the azimuthal angle ϕ_b, and therefore depend only on the magnitude of the impact vector $\mathbf{b}$. When the expansion (3.12) for the phase shift is expressed in terms of these functions we find

$$\chi(\mathbf{b},\Omega_p)=\sqrt{4\pi}\sum_{L,M}\chi_{LM}(b)e^{-iM\phi_b}Y_L^M(\Omega_p)\,. \tag{3.14}$$

The same symmetry arguments we gave before in connection with the functions $t_{LM}(b)$ now suffice to show that

$$\chi_{LM}(b)=0 \quad \text{for all odd } L,M\,, \tag{3.15a}$$

$$\chi_{L,-M}(b)=\chi_{LM}(b)\,. \tag{3.15b}$$

The evaluation of the scattering amplitude (2.2) that leads to the various nuclear rotational states requires us to resolve the nucleon profile function into its spherical harmonic components. We shall define these as

$$\Gamma_{LM}(b)=\frac{1}{\sqrt{4\pi}}e^{iM\phi_b}\int Y_L^M(\Omega_p)^\dagger\Gamma(\mathbf{b},\Omega_p)d\Omega_p\,, \tag{3.16}$$

$$\Gamma_{LM}(b)=\frac{1}{\sqrt{4\pi}}e^{iM\phi_b}\int Y_L^M(\Omega_p)^\dagger(1-e^{i\chi(\mathbf{b},\Omega_p)})d\Omega_p\,. \tag{3.17}$$

Since the phase shift $\chi(\mathbf{b},\Omega_p)$ can only depend on the difference of the azimuthal angles $\phi_b-\phi_p$, the expressions $\Gamma_{LM}(b)$ depend on the magnitude of the impact vector b alone. Since $\Gamma_{LM}(b)$ does not depend on ϕ_b, its value is not changed by reversing the sign of ϕ_b (or setting it equal to zero as we shall do later). Furthermore, the value of the integrals in Eqs. (3.16) and (3.17) is not altered by reversing the sign of the integration variable ϕ_p. The latter change, however, is equivalent (for even L) to substituting $[Y_L^{-M}(\Omega_p)]^\dagger$ for $[Y_L^M(\Omega_p)]^\dagger$. It follows then that the profile functions $\Gamma_{LM}(b)$ are even in the index M,

$$\Gamma_{L,-M}(b)=\Gamma_{LM}(b)\,. \tag{3.18}$$

By making use of the components $\Gamma_{LM}(b)$ of the profile function we can simplify appreciably the expressions for the scattering amplitudes and the various cross sections. The amplitude (2.2) for scattering to the final rotational state L, M, for example, becomes

$$F_{LM}(\mathbf{q})=\frac{ik}{2\pi}\int e^{i\mathbf{q}\cdot\mathbf{b}-iM\phi_b}\Gamma_{LM}(b)d^2b\,, \tag{3.19}$$

and by identifying a familiar integral representation[7] of the Bessel function $J_M(q)$, we can reduce this to

$$F_{LM}(\mathbf{q})=i^{M+1}e^{-iM\phi_q}k\int_0^\infty J_M(qb)\Gamma_{LM}(b)b\,db\,, \tag{3.20}$$

in which ϕ_q is the azimuthal angle of the momentum transfer $\mathbf{q}$. We may note that the angle ϕ_q is essentially arbitrary. We can choose it to be zero, or perhaps more conveniently, to be $\pi/2$, in which case the scattering amplitude reduces to

$$F_{LM}(\mathbf{q})=ik\int_0^\infty J_M(qb)\Gamma_{LM}(b)b\,db\,. \tag{3.21}$$

It is clear from this expression that the transfer to the nucleus of M units of angular momentum along the $\mathbf{k}$ direction causes the forward scattering amplitude to vanish as $q^{|M|}$. The arbitrariness of ϕ_q therefore has no effect on the forward scattering amplitude, which vanishes unless $M=0$.

The property (3.18) of the profile functions assures us, since M must be even, that the scattering amplitude also depends evenly upon M

$$F_{L,-M}(q)=F_{LM}(q)\,. \tag{3.22}$$

The integrated partial cross sections of Eq. (2.5) can now be expressed as

$$\sigma_{LM}=\int|\Gamma_{LM}(b)|^2d^2b\,. \tag{3.23}$$

These are of course, for $L>0$, the individual spherical harmonic contributions to the total variance of the profile function, which expresses the rotationally inelastic cross section given by Eq. (2.10).

IV. QUADRUPOLE DEFORMATIONS

The partial wave profile functions $\Gamma_{LM}(b)$ are defined by Eq. (3.17). When they are expressed in terms of the expansion (3.14) for its phase shift function $\chi(\mathbf{b},\Omega_p)$, the result can be conveniently written in the form

$$\Gamma_{LM}(b)=\delta_{L,0}-e^{i\chi_{00}(b)}\gamma_{LM}(b)\,, \tag{4.1}$$

in which the function $\gamma_{LM}(b)$ is given by

$$\gamma_{LM}(b)=\frac{1}{\sqrt{4\pi}}e^{iM\phi_b}\int Y_L^M(\Omega_p)^\dagger\exp\left[i\sqrt{4\pi}\sum_{L',M'}{}'\chi_{L'M'}(b)e^{-iM'\phi_b}Y_{L'}^{M'}(\Omega_p)\right]d\Omega_p\,, \tag{4.2}$$

where the sum $\sum'$ has the $L=0$ term omitted. Since $\gamma_{LM}(b)$ is independent of the azimuthal angle ϕ_b there is no loss of generality involved in setting $\phi_b=0$ and we shall do that in the work that follows. We note furthermore that since, according to Eq. (3.18), $\Gamma_{LM}(b)$ depends evenly on M, the function $\gamma_{LM}(b)$ must do so as well:

$$\gamma_{L,-M}(b)=\gamma_{LM}(b)\,. \tag{4.3}$$

To evaluate the integral (4.2), which is not in general an elementary one, we shall proceed in two stages. Since the quadrupole term is typically the dominant one, by far, in the spherical harmonic expansion (1.1) of the nuclear density, we shall begin by assuming that deformation to be the only one present and show that the integral can be evaluated for that case both accurately and simply. We shall show in a later section that the higher order deformations can then be treated by expansion in series.

When the nuclear density has only a quadrupole deformation,

$$\rho(\mathbf{r})=\rho_0(r)+\rho_2(r)P_2(\cos\Theta) , \tag{4.4}$$

only the partial wave phase shifts χ_{20} and $\chi_{22}=\chi_{2,-2}$ contribute to the integral (4.2) for $\gamma_{LM}(b)$. All angular momentum transfers are then restricted to steps in which L and M change by ± 2 or 0. The attainment of any final L state then requires at least $\frac{1}{2}L$ such steps, but the number of virtual steps involved in the transition is, in principal, unbounded. The number of virtual transitions that must be actually accounted for depends in practice on the magnitude of $\rho_2(r)$. If the nuclear surface is taken, as it is in many parametrizations, to lie at

$$r=c[1+\beta_2 Y_2^0(\cos\Theta)] , \tag{4.5}$$

in which c is the radius of a comparable sphere, then the magnitudes of $\rho_2(r)$, $\chi_{20}(b)$, and $\chi_{22}(b)$ will be governed by the deformation parameter β_2. Since $|\beta_2|$ is found in practice to have a magnitude always less than 0.35, we shall see that the number of virtual steps that must be accounted for in any rotational transition is never very large, at least not within the range of momentum transfers accessible to diffraction theory.

To begin the evaluation of $\gamma_{LM}(b)$ for the pure quadrupole case we note that it can be expressed in the form

$$\gamma_{LM}(b)=\frac{1}{\sqrt{4\pi}}\int Y_L^M(\Omega_p)^\dagger \times\exp[A(b,\mu)+B(b,\mu)\cos 2\phi_p]\,d\Omega_p , \tag{4.6}$$

where we have written $\mu=\cos\theta_p$ and

$$A(b,\mu)=i\frac{\sqrt{5}}{2}\chi_{20}(b)(3\mu^2-1) , \tag{4.7}$$

$$B(b,\mu)=i(\tfrac{15}{2})^{1/2}\chi_{22}(b)(1-\mu^2) . \tag{4.8}$$

According to Eq. (4.3), we need only evaluate this integral for $M\geq 0$. When we substitute the explicit form for $Y_L^M(\Omega_p)$, in that case we can express the integral as

$$\gamma_{LM}(b)=\frac{1}{4\pi}N_{LM} \times\int_{-1}^{1}d\mu\int_0^{2\pi}d\phi\,P_L^M(\mu)e^{-iM\phi} \times\exp[A(b,\mu)+B(b,\mu)\cos 2\phi] , \tag{4.9}$$

in which the constant N_{LM} is given by

$$N_{LM}=\left[(2L+1)\frac{(L-M)!}{(L+M)!}\right]^{1/2} . \tag{4.10}$$

The integration over the azimuthal variable ϕ can easily be carried out in closed form. A practical way to carry out the remaining integration over μ is to expand the integrand first in powers of A and B. The details of this calculation are presented in Appendix A, together with an explicit tabulation of the results for $L\leq 6$, a limit that is probably adequate for the pure quadrupole case. We shall confine ourselves here to noting that the expansion procedure we have used expresses $\gamma_{LM}(b)$ as a sum of terms proportional to $\beta_2^{L/2}$ and higher power of β_2. The individual terms of this sum are homogeneous polynomials of increasing order in the phase shift functions $\chi_{20}(b)$ and $\chi_{22}(b)$. The general form of the result can be written as

$$\gamma_{LM}(b)=N_{LM}(\tfrac{3}{4})^{M/4}\sum_{Q=L/2}^{\infty}W_{LM}(Q;\chi_{22},\chi_{20}) , \tag{4.11}$$

in which the functions W_{LM} are the Qth order homogeneous polynomials

$$W_{LM}(Q;\chi_{22},\chi_{20})=\left[\frac{i\sqrt{5}}{2}\chi_{20}\right]^{Q}\sum_{p=0}^{[(Q-M/2)/2]}\omega_{LM}(Q,p)\left[\frac{\sqrt{2}\chi_{22}}{\chi_{20}}\right]^{(M/2)+2p} \tag{4.12}$$

The coefficients ω_{LM} are a set of rational numbers that are presented for the elastic and inelastic transitions in Appendix A for $Q\leq 5$. For larger values of Q they can be calculated from Eqs. (A4) and (A9).

V. ILLUSTRATION: APPROXIMATE APPLICATION TO ^{154}Sm

In order to illustrate several features of the preceding theory let us consider an explicit application to a model nucleus. As model parameters we have chosen those of ^{154}Sm, as determined by Barlett *et al.*,[3] who discussed elastic and inelastic scattering of 800 MeV protons. Their analysis was based on a deformed, complex Woods-Saxon potential with a relatively small real part. We shall drop the real part to begin with, and take the interaction to be purely absorptive, since that makes the profile functions $\Gamma_{LM}(b)$ real, and enables us to see their properties more easily. We retain, furthermore, only the quadrupole deformation of the potential and refer to Secs. VI and VII for a discussion of the importance of higher order deformations.

The optical potential we use takes the form

$$V(\mathbf{r})=V_0(r)+V_2(r)P_2(\cos\Theta) , \tag{5.1}$$

as seen in the intrinsic coordinate system. Its spherical

component is given by

$$V_0(r)=(\mathcal{V}_0-i\mathcal{W}_0)/(1+e^{(r-c)/a}) , \tag{5.2}$$

with $\mathcal{V}_0=0$ for the moment, $\mathcal{W}_0=70$ MeV, $c=5.762$ fm, and $a=0.600$ fm. The quadrupole term, we assume, is given by

$$V_2(r)=-\beta_2 c\frac{d}{dr}V_0(r) , \tag{5.3}$$

with $\beta_2=0.301$.

Since we are beginning, in this case, by expanding the optical potential directly, rather than beginning with the density function, it is worth noting that the phase shift function can also be written as

$$\chi(\mathbf{b},\Omega_p)=-\frac{E}{\hbar^2c^2k}\int_{-\infty}^{\infty}V(\mathbf{b}+\hat{\kappa}z,\Omega_p)dz , \tag{5.4}$$

where E/c^2 is the effective relativistic mass of the proton and $\hbar k$ is its momentum. The partial wave phase shifts are then given by the expressions

$$\chi_{LM}(b)=-\frac{E}{\hbar^2c^2k}\frac{\sqrt{4\pi}}{2L+1}\times\int_{-\infty}^{\infty}V_L[(b^2+z^2)^{1/2}]Y_L^M(\theta_r,0)dz , \tag{5.5}$$

which are analogous to those of Eq. (3.4a) and have been simplified in appearances, without changing their values, by setting $\phi_b=0$.

The evaluation of the phase shift functions $\chi_{LM}(b)$ is straightforward and leads to results shown in the graphs of Fig. 1. The phase shift $-i\chi_{00}(b)$ shown in Fig. 1(a) is a measure of the integrated opacity of the nucleus as seen at impact parameter b. It takes the form one would expect for a strongly absorbing sphere with a diffuse edge. The phase shift $-i\chi_{22}(b)$ shown in Fig. 1(b) is a measure of the fluctuating part of the shadow cast by the nucleus when its angular momentum vector is aligned parallel (or antiparallel) to the incident wave vector k. The shadow does not fluctuate at all, in that case, at the central impact parameter $b=0$. Its fluctuation, and the nonzero values of $-i\chi_{22}(b)$, are confined to a ring of impact parameters or b values near the radius of the nuclear surface. The phase shift $-i\chi_{20}(b)$ shown in Fig. 1(c) gives the weighting of P_2 to the opacity fluctuations that occur as the nuclear symmetry axis spins about an axis perpendicular both to itself and to k. The result is that there is appreciable fluctuation of the opacity both at $b=0$ and at the radius of the nuclear surface.

Equipped with the values of the phase shift functions, we can use Eqs. (4.1), (4.11), and (4.12) to evaluate the profile functions $\Gamma_{LM}(b)$. These functions are interesting in their own right since their squared moduli show, according to Eq. (3.23), the distribution of impact parameters at which the various inelastic transitions take place. The calculation of these functions also gives us an opportunity to test the convergence of the expansion and we evaluate them in Appendix A. Two approximations to the function $\Gamma_{00}(b)$ are shown in Fig. 2(a). The dashed curve is the one that corresponds to taking only the spherically symmetric potential V_0 into account and setting $\gamma_{00}(b)=1$, in effect. The solid curve in Fig. 2(a) is the one that corresponds to taking full account of the deformation by summing the series for $\gamma_{00}(b)$. The difference is not great, and does not require all of the accuracy retained in the series expansion of Appendix A. The terms up to order β_2^2 are sufficient for 0.5% accuracy.

It is worth noting that taking the deformation, and thus the possibility of inelastic transitions into account, has the net effect of increasing the transparency of the nucleus in the elastic channel. The resulting decrease in $|\Gamma_{00}|^2$ leads to a decrease of the elastic scattering cross section σ_{00}. Opening the inelastic channels in this way leads, in fact, to a decrease in the total cross section as well. According to Eqs. (2.11) and (3.17) the total cross section is given by

$$\sigma_{\text{tot}}=2\,\text{Re}\int\Gamma_{00}(b)d^2b . \tag{5.6}$$

The profile function Γ_{00} is real and positive in the present case and, as shown in Fig. 2(a), is decreased in magnitude by allowing for the possibility of rotational transitions.

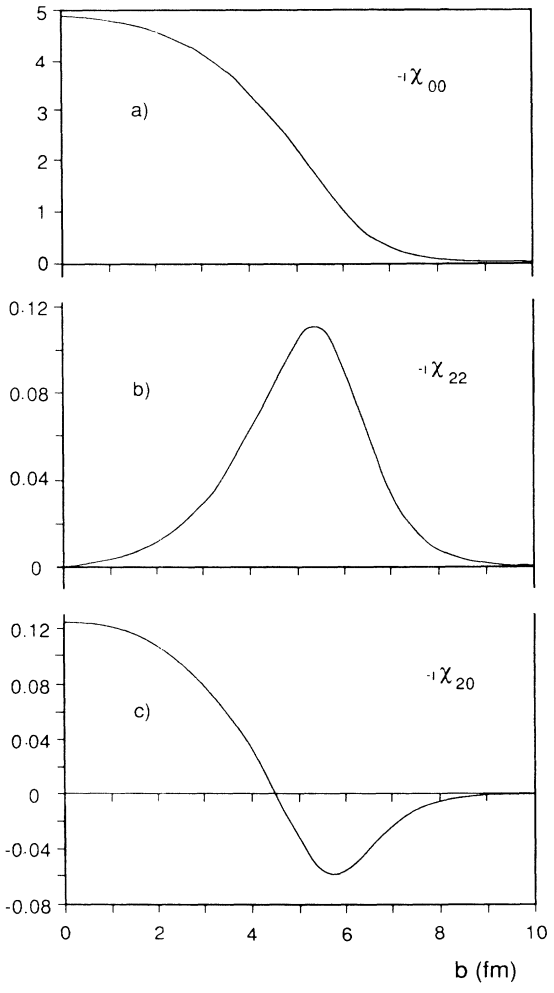

FIG. 1. The phase shift functions $-i\chi_{00}$, $-i\chi_{22}$, and $-i\chi_{20}$ for ^{154}Sm, as defined by Eq. (5.5), calculated in the quadrupole model for a purely imaginary potential.

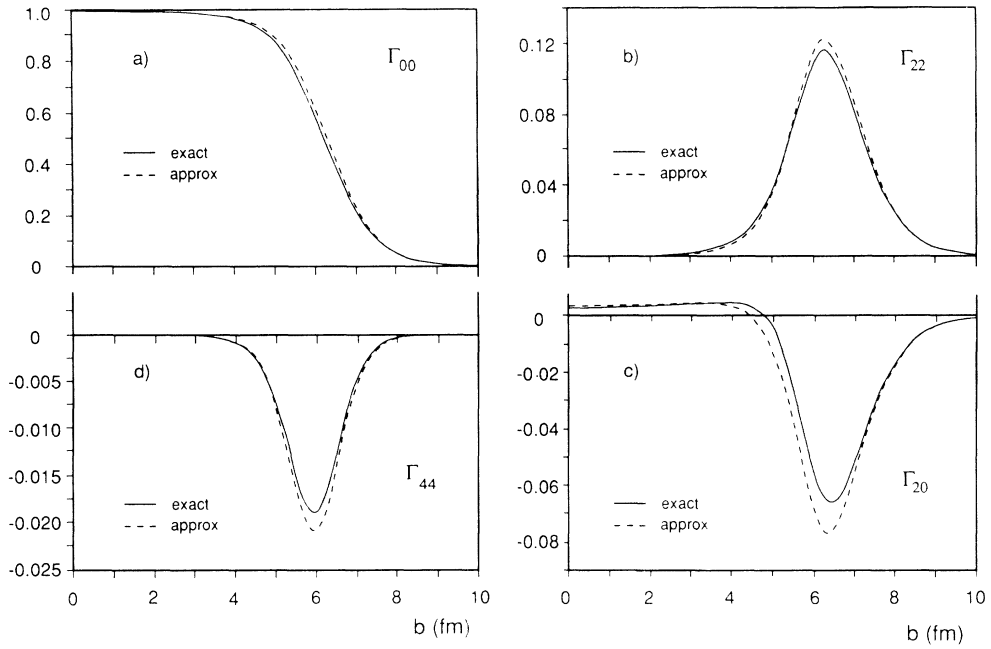

FIG. 2. Profile functions Γ_{LM} for ^{154}Sm in the quadrupole model. The dashed curves pertain to the lowest order approximation, i.e., the terms proportional to $\beta_2^{L/2}$. The solid curves include all powers of β_2 up to and including $\beta_2^{L/2+6}$. In practice, the latter curves would have been unchanged had we stopped at powers $\beta_2^{L/2+2}$.

The profile functions $\Gamma_{22}(b)$, $\Gamma_{20}(b)$, and $\Gamma_{44}(b)$ are shown in Figs. 2(b), 2(c), and 2(d), respectively. The dashed curves correspond to the lowest order approximations in powers of β_2, that is, to retaining only the first terms, of order $\beta_2^{L/2}$, in the expansions of $\gamma_{LM}(b)$. The convergence of the further terms of the series expansions is quite rapid. Taking only the terms of the next two powers of β_2 into account yields curves indistinguishable from those of the full series.

Because the opacity fluctuations associated with the transition to the 22 state are confined to a ring-shaped region in the impact plane, it is only in that region that the profile function $\Gamma_{22}(b)$, shown in Fig. 2(b), is different from zero. The fact that the nuclear symmetry axis rotates in the impact plane means that the opacity fluctuations are entirely peripheral in that case. The case of the 20 final state is somewhat different. It does indeed have opacity fluctuations at $b=0$, as we have noted, but the attenuation produced at small impact parameters by the spherical component of the potential tends to suppress their effect considerably. The graph of the resulting function $\Gamma_{20}(b)$ can be seen in Fig. 2(c) to have appreciably smaller modulus than $\Gamma_{22}(b)$. The result is that the partial cross section for the 22 final state is roughly three times larger than for the 20 final state. That behavior seems, in fact, to hold for inelastic transitions to states of higher L as well. The dominant cross section corresponds to the final states $|M|=L$ and the partial cross sections decrease with decreasing $|M|$.

It is not difficult, once we have the profile functions $\Gamma_{LM}(b)$, to evaluate the scattering amplitudes, given by Eq. (3.20). For the case of the purely absorptive interaction we have considered to this point the scattering amplitudes $F_{LM}(q)$ will all be purely imaginary and will oscillate in sign. Each of the partial cross sections will then have a succession of zeros. An optical potential that allows for refraction as well as absorption effects, that is one that has a nonvanishing real part, replaces the unrealistic zeroes by diffraction minima of the sort that are actually observed. It seems preferable at this point, before graphing the differential cross sections, to give the potential (5.2) a real part different from zero. We have chosen $\mathcal{V}_0=21.00$ MeV.

Once the optical potential is chosen to be complex, the functions plotted as Figs. 1 and 2 are no longer purely real, but the approximate conclusions we have drawn from them remain valid nontheless. The differential cross section for elastic transitions to the $L=0$ final state is shown in Fig. 3 together with the summed cross sections for inelastic transitions to the $L=2$ and $L=4$ states. The dashed curves in each case correspond to retaining only the lowest order terms, those of order $\beta_2^{L/2}$, in the expansions of $\gamma_{LM}(b)$. The solid curves represent summation of the full series.

The general shape of the elastic differential cross section does not seem to be altered appreciably by taking the deformation of the optical potential into account. It still corresponds closely in appearance to the diffraction pattern of an absorbing sphere with a diffuse surface. The differential cross section for $L=2$, on the other hand, has a rather different structure. Its strange-looking behavior near the forward direction invites explanation.

The graph presented for $L=2$ in Fig. 3 is the sum of the three differential cross sections for transitions to the final states with $M=\pm 2$ and 0. The cross sections for the final states $|M|=2$ and $M=0$ have rather different

shapes, as can be seen in Fig. 4 where they are plotted individually, along with the appropriate sum. Since the profile function $\Gamma_{22}(b)$ is larger in magnitude than $\Gamma_{20}(b)$, and contributes via two final states, the differential cross section for the $|M|=2$ transitions tends to be the dominant contribution to the summed cross section.

Since the contributions of the profile function $\Gamma_{22}(b)$ are entirely peripheral and localized to an annulus near $b=c$, the scattering amplitude $F_{22}(q)$ given by Eq. (3.20) will be roughly proportional to $J_2(qc)$. While the corresponding differential cross section, proportional to $|J_2(qc)|^2$, tends to dominate the $L=2$ summed cross section at most momentum transfers, it cannot do so near $q=0$, where it must clearly vanish as q^4.

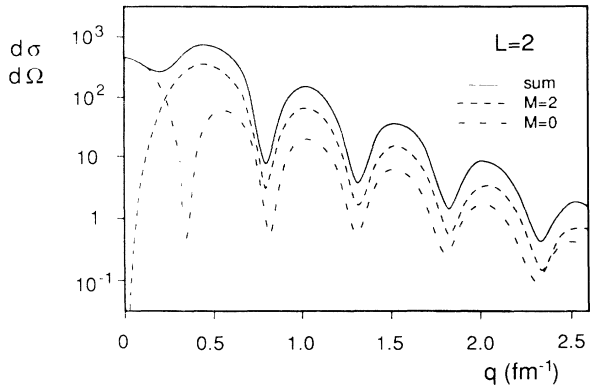

FIG. 4. The partial contributions $|F_{20}|^2$ and $|F_{22}|^2$ as well as the summed cross section $|F_{20}|^2+2|F_{22}|^2$ in the $L=2$ case. The curves plotted are calculated in the quadrupole model, summing terms up to and including order β_2^7 in the profile functions.

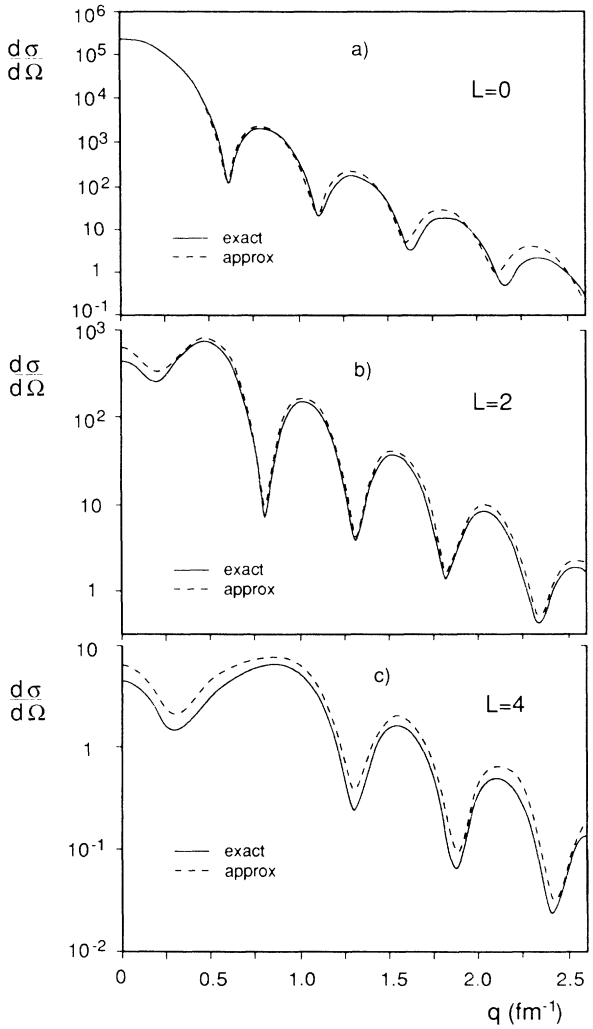

FIG. 3. Differential cross sections, in mb/sr, for ^{154}Sm in the quadrupole model. For a given final state rotational quantum number L, the curves graphed sum the contributions from all the magnetic substates. The dashed curves take into account only the lowest order contributions in powers of β_2, whereas the solid curves incorporate all contributions of powers less than or equal to $\beta_2^{L/2+6}$ in the underlying profile functions.

It is clear from the structure of the integral (3.20) that the scattering amplitude $F_{20}(q)$, on the other hand, will have a maximum modulus at $q=0$. If the profile function $\Gamma_{20}(b)$ is approximately peripheral at radius c, then the amplitude $F_{20}(q)$ is roughly proportional to $J_0(qc)$. The value of the summed differential cross section for $L=2$ is therefore contributed entirely by the $M=0$ component close to the forward direction, but then predominantly by the $M=\pm 2$ states for larger momentum transfers. It is that exchange of the dominant roles in the summed cross section that explains the strange form of the $L=2$ curve in Figs. 3 and 4. An analogous shifting of roles among the five final M states explains the form of the summed differential cross section for $L=4$ shown in Fig. 3.

VI. HIGHER ORDER MULTIPOLE DEFORMATIONS

We turn now to the treatment of axially symmetric nuclei of more general shape. According to Eq. (1.1), the expansion of the nuclear density function may contain spherical harmonics of arbitrarily high order. The phase shift function $\chi(\mathbf{b},\Omega_p)$ then becomes a sum involving spherical harmonics of similarly high order. The profile function $\gamma_{LM}(b)$ is defined by Eq. (4.2). Since it is independent of the angle ϕ_b, we can let $\phi_b=0$, so that

$$\gamma_{LM}(b)=\frac{1}{\sqrt{4\pi}}\int Y_L^M(\Omega_p)^\dagger \times\exp\left[i\sqrt{4\pi}\sum{}'\chi_{L'M'}(b)Y_{L'}^{M'}(\Omega_p)\right]d\Omega_p\ . \tag{6.1}$$

As before, $\sum'$ stands for a summation over even-ordered harmonics with $L\neq 0$.

The angular integration in Eq. (6.1) can be performed, as we have seen in the case of the quadrupole deformation, by first expanding the exponential function in series. When performing the series expansion in the present case, however, we encounter spherical harmonics of arbi-

trarily high order, and indeed products of arbitrary numbers of them. It is important to observe then that any product of spherical harmonics can be reduced to a sum of spherical harmonics, which permits the angular integration to be carried out immediately. By paying careful attention to the transformation properties of products of the spherical harmonics under rotations we can easily find an algorithm for this reduction.

The phase shift function $\chi(\mathbf{b},\Omega_p)$ depends on the angles ϕ_b and those of Ω_p. It is nevertheless invariant under rotations of the coordinate frame. This property can be made more evident by introducing the notion of a scalar product. The spherical harmonics $Y_L^M(\Omega_p)$ and the phase shift functions $\chi_{LM}(b)e^{iM\phi}$ both transform as spherical tensors under rotations of the coordinate frame. We can thus combine them by means of the Clebsch-Gordan coefficient

$$\langle LML-M|00\rangle=\frac{(-1)^{L-M}}{\sqrt{2L+1}}\ , \tag{6.2}$$

to form a scalar invariant. It is $(-1)^L(2L+1)^{1/2}$ times this invariant that we define to be the scalar product of the two tensors

$$(\chi_L\cdot Y_L)\equiv\sum_M(-1)^M\chi_{L,-M}(b)e^{-iM\phi_b}Y_L^M(\Omega_p)\ , \tag{6.3}$$

$$(\chi_L\cdot Y_L)=\sum_M\chi_{LM}(b)e^{-iM\phi_b}Y_L^M(\Omega_p)\ . \tag{6.4}$$

Comparison of this expression with the arguments of the exponential functions in Eqs. (4.2) and (6.1) (and noting that the latter has ϕ_b equal to zero) shows that these arguments are sums of scalar products $(\chi_L\cdot Y_L)$.

When we expand the exponential function in Eq. (6.1) we encounter products of scalar products. The simplest of these takes the form $(\chi_{L_1}\cdot Y_{L_1})(\chi_{L_2}\cdot Y_{L_2})$. It can be reduced by rewriting the products of the two spherical harmonics as a sum of spherical harmonics of order L, where L obeys the triangular inequality $|L_1-L_2|\le L\le L_1+L_2$. When we do this, we find that the products of the components of the tensors χ_{L_1} and χ_{L_2} occur in combinations that make it convenient to define an Lth order tensor product $(\chi_{L_1}\times\chi_{L_2})_L$ with the property

$$(\chi_{L_1}\cdot Y_{L_1})(\chi_{L_2}\cdot Y_{L_2})=\frac{1}{\sqrt{4\pi}}\sum_L[(\chi_{L_1}\times\chi_{L_2})_L\cdot Y_L]\ . \tag{6.5}$$

Once we have constructed the appropriate definition, products of several scalar products can be reduced by repeated application of Eq. (6.5).

To reach the appropriate definition for the tensor product $(\chi_{L_1}\times\chi_{L_2})_L^M$ we first note that the product of two spherical harmonics can be expanded as[8]

$$Y_{L_1}^{M_1}(\Omega)Y_{L_2}^{M_2}(\Omega)=\left[\frac{1}{4\pi}(2L_1+1)(2L_2+1)\right]^{1/2}\sum_{L,M}\begin{pmatrix}L_1 & L_2 & L_3\\ 0 & 0 & 0\end{pmatrix}\langle L_1M_1L_2M_2|LM\rangle Y_L^M(\Omega)\ . \tag{6.6}$$

In this expression use has been made of a 3-j symbol as well as the Clebsch-Gordan coefficients, and the sum over L is restricted to the values allowed by the triangular inequality. It is immediately clear then that the appropriate definition of the tensor product $(\chi_{L_1}\times\chi_{L_2})_L^M$ is

$$(\chi_{L_1}\times\chi_{L_2})_L^M\equiv[(2L_1+1)(2L_2+1)]^{1/2}\begin{pmatrix}L_1 & L_2 & L\\ 0 & 0 & 0\end{pmatrix}\times\sum_{M_1,M_2}\langle L_1M_1L_2M_2|LM\rangle\chi_{L_1}^{M_1}\chi_{L_2}^{M_2}\ . \tag{6.7}$$

This definition, furthermore, has the simple properties

$$(\chi_L\times Y_L)_0^0=(\chi_L\cdot Y_L) \tag{6.8}$$

and

$$(\chi_L\times Y_0)_L^M=(-1)^L\chi_{LM}Y_0^0\ . \tag{6.9}$$

The reduction of the expanded exponential function can now be achieved by making repeated use of the identity (6.5) and the definition (6.7). The result we obtain takes the form

$$\exp\left[i\sqrt{4\pi}\sum_L(\chi_L\cdot Y_L)\right]=1+i\sqrt{4\pi}\sum_{L_1}(\chi_{L_1}\cdot Y_{L_1})-\frac{1}{2!}\sqrt{4\pi}\sum_{L_1,L_2,L_{12}}[(\chi_{L_1}\times\chi_{L_2})_{L_{12}}\cdot Y_{L_{12}}]+\cdots\ . \tag{6.10}$$

There are of course other orders of procedure in which the reduction can be accomplished. The exponential function could, for example, be factorized first and each of the factors reduced before they are all combined. Such procedures will lead to the occurrence of different tensor products in the intermediate stages, but the final result of all the reductions must be the same. Once the exponential function is fully reduced in this way, the integrand in Eq. (6.1) involves only bilinear products of spherical harmonic functions. The angular integrations can then be carried out immediately. Since the phase shift functions $\chi_{LM}(b)$ are different from zero only for even values of L and M we find that the profile functions $\gamma_{LM}(b)$ can be written as

$$\gamma_{LM}(b)=\gamma_{L,-M}(b)=\delta_{L,0}+i\chi_{LM}+\frac{1}{2!}i^2\sum_{L_1,L_2}(\chi_{L_1}\times\chi_{L_2})_L^M+\frac{1}{3!}i^3\sum_{\substack{L_1,L_2,L_3\\ L_{12}}}[(\chi_{L_1}\times\chi_{L_2})_{L_{12}}\times\chi_{L_3}]_L^M+\cdots\ . \tag{6.11}$$

This is the series we shall eventually sum in order to evaluate the profile function. It can be expressed by the simple mnemonic

$$\gamma_{LM}(b)=\left\{\exp\left[i\sum_{L'}{}'\chi_{L'}(b)\right]\right\}_L^M , \tag{6.12}$$

which is understood to have the expansion (6.11). We could, of course, have used the expansion in this form to discuss the case of the quadrupole deformation of Sec. IV. Only two phase shift functions χ_{22} and χ_{20}, were required for that case, however, and it thus seemed simpler to proceed more directly.

An elementary property of the profile functions and tensor products we have discussed greatly simplifies the calculations when higher order deformations are added to the potential. Let us suppose that the phase shift function is the sum of two terms,

$$\chi(\mathbf{b},\Omega)=\chi^{(1)}(\mathbf{b},\Omega)+\chi^{(2)}(\mathbf{b},\Omega) , \tag{6.13}$$

and that the function $\gamma^{(1)}_{LM}(b)$ and $\gamma^{(2)}_{LM}$ are the corresponding profile functions, defined by Eqs. (4.2) or (6.1). Then the profile function tensor $\gamma(b)$ that corresponds to the sum (6.13) is given mnemonically by the product $\gamma(b)=\gamma^{(1)}(b)\gamma^{(2)}(b)$; that is to say we have

$$\gamma_{LM}(b)=\sum_{L_1,L_2}[\gamma^{(1)}_{L_1}(b)\times\gamma^{(2)}_{L_2}(b)]^M_L , \tag{6.14}$$

in which the sum is carried out over all angular momenta L_1 and L_2 that can sum to L.

In order to prove the identity (6.14) we first note that Eq. (6.10) can be written more compactly as

$$\exp[i\chi(\mathbf{b},\Omega)]=\sqrt{4\pi}\sum_L[\gamma_L(b)\cdot Y_L(\Omega)] . \tag{6.15}$$

Then if $\chi(\mathbf{b},\Omega_p)$ is the sum of two terms, as in Eq. (6.13), we can factorize the exponential and apply the identity to each of the factors. We then have

$$\begin{aligned}\exp[i\chi(\mathbf{b},\Omega)]&=4\pi\sum_{L_1,L_2}[\gamma^{(1)}_{L_1}(b)\cdot Y_{L_1}(\Omega)][\gamma^{(2)}_{L_2}(b)\cdot Y_{L_1}(\Omega)]\\&=\sqrt{4\pi}\sum_{L'}\left\{\sum_{L_1,L_2}\{[\gamma^{(1)}_{L_1}(b)\times\gamma^{(2)}_{L_2}(b)]_{L'}\cdot Y_{L'}(\Omega)\}\right\} .\end{aligned} \tag{6.16}$$

This relation again falls into the form of Eq. (6.15), but with the compound profile function given, as we have stated, by the identity (6.14).

The multiplicative rule (6.14) is quite helpful in taking into account the corrections due to higher order deformations. Let us assume, for example, that, as in the preceding section, the profile functions for the case of pure quadrupole deformation have already been determined. Then we may treat the hexadecapole (2^4-pole) and the hexekontatettarapole (2^6-pole) deformations by using the multiplication rule as the basis for a series expansion. Let us write the $L=0$ part of the phase shift in terms of the spherical harmonic components as $\chi_2+\chi_4+\chi_6$. We assume that we already know the profile tensor for the phase shift χ_2 and shall call it $\bar{\gamma}_{LM}(b)$. Then the full tensor can be written, according to Eq. (6.14), in the abbreviated form

$$\gamma_L=\sum_{L_1,L_2}\{[1+i\chi_4+i\chi_6-\tfrac{1}{2}(\chi_4\times\chi_4)+\cdots]_{L_1}\times\bar{\gamma}_{L_2}\}_L . \tag{6.17}$$

The only terms of the sum on the right that can contribute, of course, are those that satisfy the triangle inequality.

Let us assume now, that the phase shift functions χ_L are of order $\varepsilon^{L/2}$, where ε is a small deformation parameter of some sort. Then the correction terms of any order in ε to the profile functions $\bar{\gamma}_{LM}(b)$ may be found from the expansion (6.17). When we include corrections of order ε^2 we find, for example, for

$$L=0:\ \gamma_0=\bar{\gamma}_0 , \tag{6.18a}$$

$$L=2:\ \gamma_2=\bar{\gamma}_2+i(\chi_4\times\bar{\gamma}_2)_2 , \tag{6.18b}$$

$$L=4:\ \gamma_4=\bar{\gamma}_4+i[\chi_4\times(\bar{\gamma}_0+\bar{\gamma}_2+\bar{\gamma}_4)+\chi_6\times\bar{\gamma}_2]_4-\tfrac{1}{2}(\chi_4\times\chi_4)_4\bar{\gamma}_0 . \tag{6.18c}$$

If we wish to retain powers of ε no higher than $\frac{1}{2}L+2$, of course, some of the expressions for $\bar{\gamma}_{LM}(b)$ in these equations should be appropriately truncated.

VII. APPLICATION INCLUDING HIGHER ORDER DEFORMATIONS

We now apply our formalism to a more complete picture of the nucleus ^{154}Sm. The model parameters are again chosen from Bartlett *et al.*[3] The optical potential is assumed to be given in the body-fixed system by a deformed Woods-Saxon function:

$$V(\mathbf{r})=(\mathcal{V}_0-i\mathcal{W}_0)/(1+\exp\{[r-R(\Theta)]/a\}) , \tag{7.1}$$

with

$$R(\Theta)=c\left[1+\sum_{L=2,4,\ldots}\beta_L Y_L^0(\Theta)\right]. \tag{7.2}$$

We shall limit ourselves, in the present calculations, to studying the excitation of the $L=2$ and $L=4$ final states by means of the approximation given by Eq. (6.18). The additional parameters[3] we require are then $\beta_4=0.110$ and $\beta_6=-0.016$.

The potential $V(\mathbf{r})$ must now be expanded in spherical harmonics, but we can no longer be satisfied with retaining only the second harmonic term as we were in Eq. (5.1). The more complete expansion is developed in Appendix B, where each spherical harmonic term, $V_{LM}(r)$, is seen to contain several powers of β_2 as well as certain of the higher order β_L's.

If we again let $\mathcal{V}_0=0$ for the moment, and take the potential to be purely absorptive, the profile functions $\Gamma_{LM}(b)$ become real valued, and we can display them graphically. The results for the dominant profile functions $\Gamma_{22}(b)$ and $\Gamma_{44}(b)$ are shown in Figs. 5(a) and 5(b), respectively. It is clear from both of these graphs that taking the higher order effects of deformation into account slows the convergence of the expansions we have been using. Furthermore, the magnitude and shape of the profile function $\Gamma_{44}(b)$ has been changed quite drastically from the form it took for the pure quadrupole deformation, in Fig. 2(d).

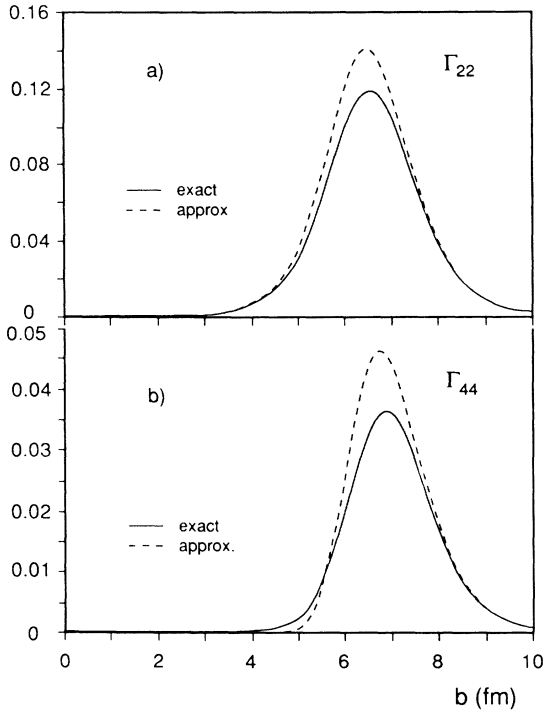

FIG. 5. Profile functions Γ_{22} and Γ_{44} calculated in the model that also includes β_4 and β_6 deformations. The dashed curves take into account only the β_2 deformation and in the case of Γ_{44} the β_4 deformation, but only in lowest order. The solid curves are the complete results that sum all terms of orders less than or equal to $\varepsilon^{L/2+3}$ in the notation of Eq. (6.18).

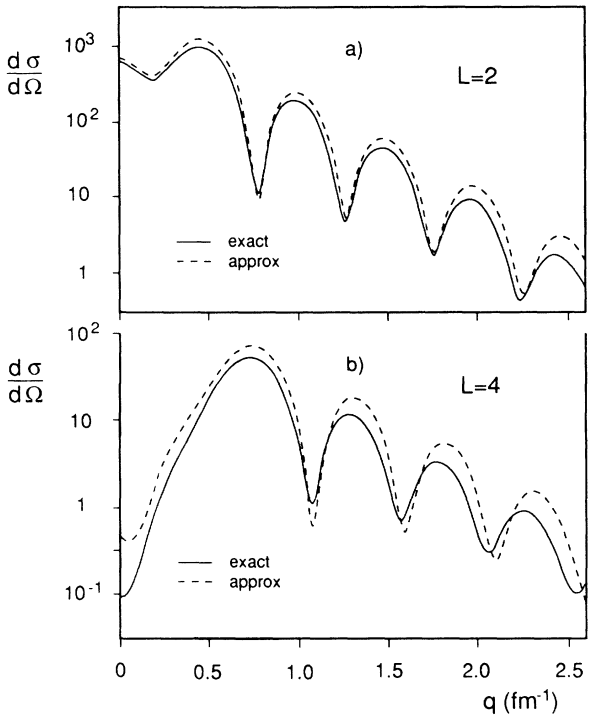

FIG. 6. Differential cross sections, summed over magnetic substates, for $L=2$ and 4 calculated with inclusion of the β_2 and β_4 deformations. The dashed curves are derived from profile functions that are independent of β_4 and β_6 for $L=2$ and include β_4 only linearly for $L=4$. The solid curves are based on profile functions that sum all terms of order less than or equal to $\varepsilon^{L/2+3}$.

We present in Fig. 6 the summed differential cross sections for the final states of angular momentum $L=2$ and $L=4$, calculated with all of the parameters stated, but with the real part of the potential restored to the value $\mathcal{V}_0=21.00$ MeV. By comparing these graphs with Fig. 3, we can see that taking the higher order deformations into account changes the shape of both differential cross sections. For the case $L=4$ the change is a dramatic one in magnitude as well as shape. We expect analogous results to hold for all of the higher order rotational transitions.

VIII. A PERIPHERAL APPROXIMATION

In an interesting recent paper Ginocchio, Otsuka, Amado, and Sparrow[6] have discussed hadron-nucleus scattering by means of the interacting boson model. They have applied the model within the context of diffraction theory and have proposed an important simplification of the expressions for the case of strongly absorbing nuclei. The particles that are in the scattered wave, they assumed, have all collided with the nucleus more or less peripherally, that is to say in a region of small $|z|$. Since we have a more complete theory at hand, it is of value to investigate the accuracy of this approximation.

We can calculate the phase shifts $\chi_{LM}(b)$ in this ap-

proximation quite simply from Eq. (5.5). We have only to substitute the fixed value $\theta_r=\pi/2$ in the argument of $Y_L^M(\theta_r,0)$, which can then be factorized out of the integrand. The result can be written in the form

$$\chi_{LM}(b)=\frac{\sqrt{4\pi}}{2L+1}g_L(b)Y_L^M\left[\frac{\pi}{2},0\right], \tag{8.1}$$

where

$$g_L(b)=-\frac{E}{\hbar^2c^2k}\int_{-\infty}^{\infty}V_L[(b^2+z^2)^{1/2}]dz\ . \tag{8.2}$$

These relations imply, if taken literally, that the phase shifts $\chi_{LM}(b)$ for different M values and fixed L differ only by constant factors. It is evident, for example, from the form of $\chi_{22}(b)$ and $\chi_{20}(b)$ in Figs. 1(b) and 1(c), that these functions differ considerably in their b dependence for small b values. The approximation is only proposed for the case of strong absorption, however, and the result of the absorption will be to attenuate the effect of such differences for small b.

The total phase shift function $\chi(\mathbf{b},\Omega_p)$ can now be found from Eq. (3.14). We write it in the form

$$\begin{aligned}\chi(\mathbf{b},\Omega_p)&=\sqrt{4\pi}\sum_{L,M}(-1)^M\chi_{L,-M}(b)e^{-iM\phi_b}Y_L^M(\Omega_p)\\&=\sum_{L,M}(-1)^M\frac{4\pi}{2L+1}\\&\quad\times g_L(b)Y_L^{-M}\left[\frac{\pi}{2},0\right]e^{-iM\phi_b}Y_L^M(\Omega_p)\\&=\sum_L\frac{4\pi}{2L+1}g_L(b)\sum_M Y_L^M\left[\frac{\pi}{2},\phi_b\right]^{\dagger}Y_L^M(\Omega_p)\ .\end{aligned} \tag{8.3}$$

The sum over M may now be carried out by means of the addition theorem, Eq. (3.2). It is convenient at this point to denote the angle between the symmetry axis Ω_p and the impact vector $\mathbf{b}$ by θ_{pb}. We can then write the result for the phase shift as

$$\chi(\mathbf{b},\Omega_p)=\sum_L g_L(b)P_L(\cos\theta_{pb})\ . \tag{8.4}$$

The profile function $\Gamma_{LM}(b)$, according to Eqs. (4.1) and (4.2), is determined by the function $\gamma_{LM}(b)$, which takes the form

$$\gamma_{LM}(b)=\frac{1}{\sqrt{4\pi}}\int Y_L^M(\Omega_p)^{\dagger}\times\exp\left[i\sum_{L'}g_{L'}(b)P_{L'}(\cos\theta_{pb})\right]d\Omega_p\ . \tag{8.5}$$

Since $\gamma_{LM}(b)$ is independent of the azimuthal angle ϕ_b, as noted earlier, we have set it equal to zero in this expression. We next note that the exponential function in the integrand depends only on $\cos\theta_{pb}$. If we let

$$F(\mu)=\exp\left[i\sum_L g_L P_L(\mu)\right], \tag{8.6}$$

then we can expand $F(\mu)$ in terms of Legendre polynomials as

$$F(\mu)=\sum_L F_L P_L(\mu)\ , \tag{8.7}$$

where

$$F_L=\frac{2L+1}{2}\int_{-1}^{1}F(\mu)P_L(\mu)d\mu\ . \tag{8.8}$$

To evaluate $\gamma_{LM}(b)$ then we need only consider integrals of the form

$$\int Y_L^M(\Omega_p)^{\dagger}P_{L'}(\cos\theta_{pb})d\Omega\ . \tag{8.9}$$

We can evaluate these by using the addition theorem once again to write

$$P_{L'}(\cos\theta_{pb})=\frac{4\pi}{2L'+1}\sum_{M'}Y_{L'}^{M'}(\Omega_p)Y_{L'}^{M'}\left[\frac{\pi}{2},0\right]^{\dagger}\ . \tag{8.10}$$

The integral (8.9) is then seen to vanish unless $L'=L$ and $M'=M$. Its value is just

$$\frac{4\pi}{2L+1}Y_L^M\left[\frac{\pi}{2},0\right]^{\dagger}\delta_{LL'}\delta_{MM'}\ , \tag{8.11}$$

and the function $\gamma_{LM}(b)$ is thus given by

$$\gamma_{LM}(b)=\frac{\sqrt{4\pi}}{2L+1}Y_L^M\left[\frac{\pi}{2},0\right]^{\dagger}F_L(b)\ , \tag{8.12}$$

$$\gamma_{LM}(b)=(-1)^{(L+M)/2}\frac{1}{\sqrt{2L+1}}\times\frac{[(L-M)!(L+M)!]^{1/2}}{2^L[\frac{1}{2}(L-M)]![\frac{1}{2}(L+M)]!}F_L(b)\ . \tag{8.13}$$

This approximate result shows a property we have noted for the phase shifts earlier. The functions $\gamma_{LM}(b)$ for different values of M and fixed L are found to differ by constant factors. If Eq. (8.13) is to hold for $L=2$, for example, we should expect to find $\gamma_{20}(b)=-(\frac{2}{3})^{1/2}\gamma_{22}(b)$ and the same relation between $\Gamma_{20}(b)$ and $\Gamma_{22}(b)$. A comparison with the calculations graphed in Figs. 2(b) and 2(c) and the peripheral approximation is made in Figs. 7(a) and 7(b). The solid curves are identical to those of Figs. 2(b) and 2(c) and the dashed curves are the predictions of the peripheral approximation summed to the same order. The effect of the absorption by the central potential is to give the functions $\Gamma_{20}(b)$ and $\Gamma_{22}(b)$ roughly comparable shapes (apart from a negative factor). They fail, however, to obey the approximate identity (8.13) in the peripheral region by about 30–50%. The approximation works best for $\Gamma_{22}(b)$ where the size of the error in the peripheral approximation is comparable to the size of the higher order β_2 corrections to the lowest order profile function. These features are equally true for larger L values. The peripheral approximation works well for $|M|=L$ but deteriorates with decreasing M value.

While the functions $\Gamma_{LM}(b)$ for fixed L are found to show a common b dependence for all M values, their cor-

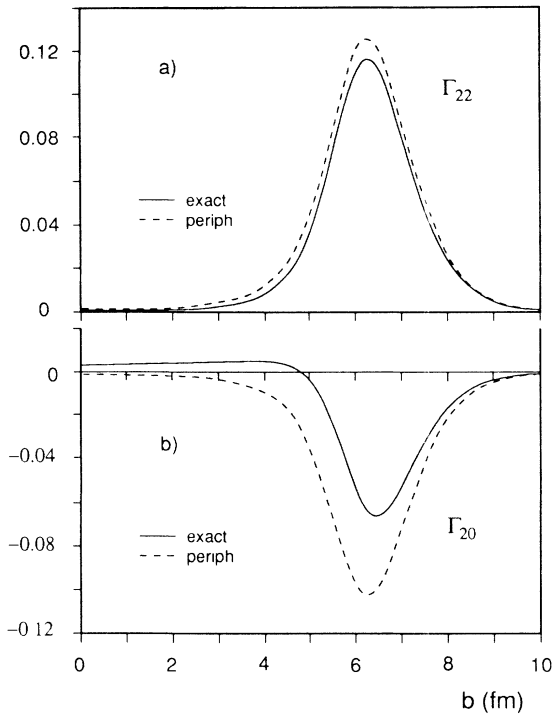

FIG. 7. The profile functions Γ_{20} and Γ_{22} in the quadrupole model. The solid curves graph the exact result, i.e., they include all terms of orders less than or equal to β_2^7, whereas the dashed curves are based on the peripheral approximation evaluated to the same order.

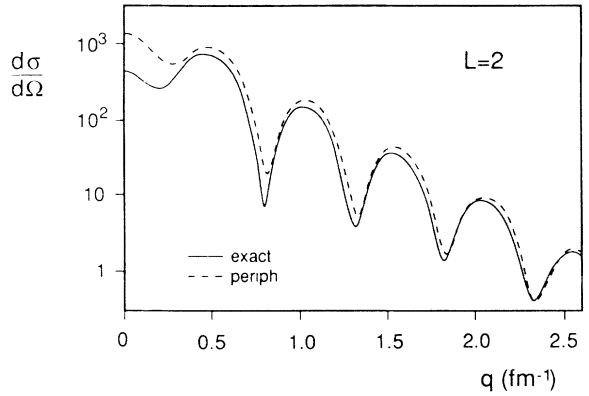

FIG. 8. Differential cross sections for $L=2$ in the quadrupole model. The solid curves show the exact results, i.e., they include terms up to order β_2^7 in the underlying profile functions, and the dashed curves show the corresponding cross sections in the peripheral approximation.

responding inelastic scattering amplitudes $F_{LM}(q)$ will all differ in shape, according to Eq. (3.20), because of the M dependence of the Bessel function $J_M(qb)$. The cross section for $L=2$ predicted by the peripheral approximation is in Fig. 8 graphed together with the exact one of Fig. 3(b). At small momentum transfers, where the contribution from $F_{20}(q)$ dominates, the peripheral approximation does not fare very well. At larger momentum transfers $F_{22}(q)$ dominates and the approximation becomes more reliable. The effect of the approximation is mainly to produce a shift in the diffraction pattern towards larger momentum transfers, implying a shrinking of the effective nuclear radius.

ACKNOWLEDGMENTS

Our work has benefited greatly from conversations we have had with Norton Hinz. We have carried it out mainly during reciprocal visits to the Lyman Laboratory at Harvard and the Gustaf Werner Institute at Uppsala, and we are grateful for the hospitality extended by both institutions. It was supported in part by the U.S. Department of Energy under Contract No. DEAC 0276 ERO-3064 and by the Swedish National Science Research Council.

APPENDIX A

The profile function $\gamma_{LM}(b)$, with $M \geq 0$, is, for the case of quadrupole deformations, given by Eq. (4.9), i.e.,

$$\gamma_{LM}(b)=\frac{1}{4\pi}N_{LM} \times \int_{-1}^{1} d\mu \int_{0}^{2\pi} d\phi\, P_L^M(\mu) e^{-iM\phi} \times \exp[A(b,\mu)+B(b,\mu)\cos 2\phi] \,. \tag{4.9}$$

The numerical factor N_{LM} is defined by Eq. (4.10) and the functions A and B by Eqs. (4.7) and (4.8),

$$A(b,\mu)=i\frac{\sqrt{5}}{2}\chi_{20}(b)(3\mu^2-1) \,, \tag{4.7}$$

$$B(b,\mu)=i(\tfrac{15}{2})^{1/2}\chi_{22}(b)(1-\mu^2) \,. \tag{4.8}$$

We perform the integrations in Eq. (4.9) by making an expansion in series in A and B. In this expansion we want to group together terms of the same power of the deformation parameter β_2. Since $\chi_{20}(b)$ and $\chi_{22}(b)$ are linear functions of β_2 this means that terms with equal sum of the powers of A and B should be assembled together. We therefore write the expansion as

$$\gamma_{LM}(b)=\frac{1}{4\pi}N_{LM}\sum_{Q=0}^{\infty}\frac{1}{Q!}\sum_{q=0}^{Q}\binom{Q}{q}\int_{-1}^{1} d\mu\, P_L^M(\mu) A(b,\mu)^{Q-q} B(b,\mu)^q \int_0^{2\pi} d\phi\, e^{-iM\phi}(\cos 2\phi)^q \,, \tag{A1}$$

where Q is the power of β_2. The possible values taken by Q and q are restricted by angular momentum coupling rules. Since A and B are functions of angular momentum 2 we need at least $L/2$ steps to reach a final state of angular momentum L starting from an initial one of angular momentum zero. Hence, all terms in Eq. (A1) that do not satisfy

the inequality $Q \geq L/2$ must necessarily vanish. Similarly, since A is a function of magnetic quantum number zero and B a linear combination of functions of magnetic quantum numbers ± 2, we need at least $M/2$ steps to reach a final state of magnetic quantum number M.

The integration over the ϕ variable in Eq. (A1) is easily carried out,

$$\frac{1}{2\pi}\int_0^{2\pi} d\phi\, e^{-iM\phi}(\cos 2\phi)^q = \frac{1}{2^q}\begin{bmatrix} q \\ \frac{1}{2}(q+M/2) \end{bmatrix} . \tag{A2}$$

The integral vanishes unless $q \geq M/2$ and $\frac{1}{2}(q+M/2)$ is an integer. It is therefore convenient to write $q = M/2+2p$, where p is a non-negative integer. Since furthermore according to Eq. (A1) we have $q \leq Q$, it follows that

$$q = \frac{M}{2} + 2p \text{ with } p = 0, 1, \ldots, \tfrac{1}{2}(Q - M/2) , \tag{A3}$$

where the bracket notation signifies the integer part of $\frac{1}{2}(Q-M/2)$. This number is always positive since $Q \geq L/2 \geq M/2$.

We now introduce the functions W_{LM} and ω_{LM} as defined by Eqs. (4.11) and (4.12):

$$\gamma_{LM}(b) = N_{LM}(\tfrac{3}{4})^{M/4} \sum_{Q=L/2}^{\infty} W_{LM}(Q;\chi_{22},\chi_{20}) , \tag{4.11}$$

$$W_{LM}(Q;\chi_{22},\chi_{20}) = \left[\frac{i\sqrt{5}}{2}\chi_{20}\right]^Q \sum_{p=0}^{[(Q-M/2)/2]} \omega_{LM}(Q,p)\left[\frac{\sqrt{2}\chi_{22}}{\chi_{20}}\right]^{(M/2)+2p} . \tag{4.12}$$

By combining these definitions with Eqs. (A1) and (A2), we conclude that

$$\omega_{LM}(Q,p) = (\tfrac{3}{4})^p \frac{1}{Q!}\begin{bmatrix} Q \\ M/2+2p \end{bmatrix}\begin{bmatrix} M/2+2p \\ M/2+p \end{bmatrix} G_{LM}\left[Q - \frac{M}{2} - 2p, \frac{M}{2} + 2p\right] , \tag{A4}$$

where the functions $G_{LM}(s,t)$ are defined by the integral

$$G_{LM}(s,t) = \tfrac{1}{2}\int_{-1}^{1} d\mu\, P_L^M(\mu)(3\mu^2-1)^s(1-\mu^2)^t . \tag{A5}$$

We have found it most convenient to evaluate the function $G_{LM}(s,t)$ by expressing the associated Legendre polynomials $P_L^M(\mu)$ as polynomials in $\sin^2\theta$ rather than the usual $\cos^2\theta$. Since in our case both L and M are even, we can write

$$P_L^M(\mu) = \sum_{k=0}^{(L-M)/2} h_{LM}(k)(1-\mu^2)^{L/2-k} . \tag{A6}$$

In particular, we observe that for $M = L$ the sum reduces to a single term. The coefficients $h_{LM}(k)$ are rational numbers. We have calculated them by using the algebraic manipulation program *SMP*. The function $G_{LM}(s,t)$ is nonzero only if $(s+t) \geq L/2$. This property follows from a partial integration of Eq. (A5) by using the expression

$$P_L^M(\mu) = (\text{const})(1-\mu^2)^{M/2}\frac{d^{L+M}}{d\mu^{L+M}}(1-\mu^2)^L . \tag{A7}$$

It leads to the restriction $Q \geq L/2$ for the function $\omega_{LM}(Q,p)$, a condition that has already been noted.

For the evaluation of the integral of Eq. (A5) we need the relation

$$\tfrac{1}{2}\int_{-1}^{1} d\mu(1-\mu^2)^m = \frac{(2m)!!}{(2m+1)!!} , \tag{A8}$$

which, together with an expansion of $(3\mu^2-1)^s$ as polynomial in $(1-\mu^2)$, leads to the expression

$$G_{LM}(s,t) = 2^s \sum_{m=0}^{s}\begin{bmatrix} s \\ m \end{bmatrix}\left[-\frac{3}{2}\right]^m \sum_{k=0}^{(L-M)/2} h_{LM}(k)\frac{(L-2k+2m+2t)!!}{(L-2k+2m+2t+1)!!} . \tag{A9}$$

Below we list the first few profile functions $\gamma_{LM}(b)$. For convenience we write the expansions in terms of the variables

$$x = i\sqrt{5/2}\chi_{22}(b) , \tag{A10a}$$

$$y = i\frac{\sqrt{5}}{2}\chi_{20}(b) . \tag{A10b}$$

We limit ourselves to those terms of Eq. (4.11) that satisfy $L/2 \leq Q \leq 5$:

$$\gamma_{00}=X_{00}[1+\tfrac{2}{5}(x^2+y^2)+\tfrac{8}{105}(-3x^2y+y^3)+\tfrac{2}{35}(x^2+y^2)^2+\tfrac{16}{1155}(x^2+y^2)(-3x^2y+y^3)] , \tag{A11}$$

$$\gamma_{20}=X_{20}[\tfrac{2}{5}y+\tfrac{4}{35}(-x^2+y^2)+\tfrac{4}{35}y(x^2+y^2)+\tfrac{8}{1155}(-3x^4-3x^2y^2+5y^4)+\tfrac{4}{15015}(69x^4y+58x^2y^3+53y^5)] , \tag{A12}$$

$$\gamma_{22}=X_{22}[\tfrac{8}{5}x-\tfrac{32}{35}xy+\tfrac{16}{35}x(x^2+y^2)-\tfrac{128}{1155}(3x^3y+xy^3)+\tfrac{16}{15015}(45x^5+138x^3y^2+29xy^4)] , \tag{A13}$$

$$\gamma_{40}=X_{40}[\tfrac{2}{105}(x^2+6y^2)+\tfrac{16}{1155}(-4x^2y+3y^3)+\tfrac{4}{15015}(27x^4+89x^2y^2+102y^4)+\tfrac{16}{45045}(-27x^4y-23x^2y^3+24y^5)] , \tag{A14}$$

$$\gamma_{42}=X_{42}[\tfrac{16}{7}xy-\tfrac{32}{77}(x^3+xy^2)+\tfrac{32}{1001}(19x^3y+11xy^3)-\tfrac{64}{3003}(3x^5+12x^3y^2+xy^4)] , \tag{A15}$$

$$\gamma_{44}=X_{44}[\tfrac{64}{3}x^2-\tfrac{512}{33}x^2y+\tfrac{128}{429}(15x^4+23x^2y^2)-\tfrac{512}{1287}(9x^4y+5x^2y^3)] , \tag{A16}$$

$$\gamma_{60}=X_{60}[\tfrac{12}{1001}(x^2y+2y^3)-\tfrac{8}{5005}(x^4+9x^2y^2-6y^4)+\tfrac{8}{85085}(41x^4y+39x^2y^3+54y^5)] , \tag{A17}$$

$$\gamma_{62}=X_{62}[\tfrac{16}{143}(x^3+12xy^2)-\tfrac{64}{143}x^3y+\tfrac{32}{2431}(3x^5+23x^3y^2+12xy^4)] , \tag{A18}$$

$$\gamma_{64}=X_{64}[\tfrac{5760}{143}x^2y-\tfrac{768}{143}(x^4+3x^2y^2)+\tfrac{768}{2431}(29x^4y+21x^2y^3)] , \tag{A19}$$

$$\gamma_{66}=X_{66}[\tfrac{7680}{13}x^3-\tfrac{6144}{13}x^3y+\tfrac{1536}{221}(14x^5+30x^3y^2)] . \tag{A20}$$

In these formulas the factor X_{LM} is defined by

$$X_{LM}=\left[(2L+1)\frac{(L-M)!}{(L+M)!}\right]^{1/2}(\tfrac{1}{4})^{M/4} . \tag{A21}$$

APPENDIX B

The deformed Woods-Saxon optical potential is defined in the body-fixed coordinate system by

$$V(\mathbf{r})=(\mathcal{V}_0-i\mathcal{W}_0)/(1+\exp\{[r-R(\Theta)]/a\}) \tag{B1}$$

with

$$R(\Theta)=c\left[1+\sum_L \beta_L Y_L^0(\Theta)\right] , \tag{B2}$$

where the sum runs only over even values of L. We have employed the potential determined by Barlett *et al.*[3] with one exception: the radial dependences of the real and imaginary parts of the potential $V(\mathbf{r})$ have been taken to be identical. As a consequence of this simplification it has been necessary to increase the depth of the real part of the potential. The following parameter values, appropriate for ^{154}Sm, have been used: $\mathcal{V}_0=21.00$ MeV, $\mathcal{W}_0=70.0$ MeV, $c=5.762$ fm, $a=0.600$ fm, $\beta_2=0.301$, $\beta_4=0.110$, and $\beta_6=-0.016$.

If we expand the optical potential in powers of the deformation parameters it can be written in the form

$$V(\mathbf{r})=V_0(r)+\sum_{L=2,4,\ldots}\left[\frac{4\pi}{2L+1}\right]^{1/2}V_L(r)Y_L^0(\Theta) . \tag{B3}$$

We shall retain in this expansion the contributions V_0, V_2, V_4, and V_6. The functional dependence on β_2 is accounted for up to and including powers β_2^3.

We define

$$E_0=1/\{1+\exp[(r-c)/a]\} , \tag{B4a}$$

$$E_1=E_0(1-E_0)/a , \tag{B4b}$$

$$E_2=E_1(1-2E_0)/a , \tag{B4c}$$

$$E_3=E_1(1-6E_0+6E_0^2)/a^2 , \tag{B4d}$$

and

$$\bar{\beta}_L=c\left[\frac{2L+1}{4\pi}\right]^{1/2}\beta_L . \tag{B5}$$

In terms of these functions the partial wave radial potentials V_L of Eq. (B3) become

$$V_0(r)=(\mathcal{V}_0-i\mathcal{W}_0)(E_0+\tfrac{1}{10}\bar{\beta}_2^2E_2+\tfrac{1}{105}\bar{\beta}_2^3E_3)\ , \tag{B6a}$$

$$V_2(r)=(\mathcal{V}_0-i\mathcal{W}_0)(\bar{\beta}_2E_1+\tfrac{1}{7}\bar{\beta}_2^2E_2+\tfrac{2}{7}\bar{\beta}_4\bar{\beta}_2E_2+\tfrac{1}{14}\bar{\beta}_2^3E_3)\ , \tag{B6b}$$

$$V_4(r)=(\mathcal{V}_0-i\mathcal{W}_0)(\bar{\beta}_4E_1+\tfrac{9}{35}\bar{\beta}_2^2E_2+\tfrac{20}{77}\bar{\beta}_2\bar{\beta}_4E_2+\tfrac{18}{385}\bar{\beta}_2^3E_3)\ , \tag{B6c}$$

$$V_6(r)=(\mathcal{V}_0-i\mathcal{W}_0)(\bar{\beta}_6E_1+\tfrac{5}{11}\bar{\beta}_2\bar{\beta}_4E_2+\tfrac{3}{77}\bar{\beta}_2^3E_3)\ . \tag{B6d}$$

[1]T. Cooper, W. Bertozzi, J. Heisenberg, S. Kowalski, W. Turchinetz, C. Williamson, L. Cardman, S. Fivozinsky, J. Lightbody, Jr., and S. Penner, Phys. Rev. C **13**, 1083 (1976); L. S. Cardman, D. H. Dowell, R. L. Gulbranson, D. G. Ravenhall, and R. C. Mercer, *ibid.* **18**, 1388 (1978).

[2]D. L. Hendrie, N. K. Glendenning, B. G. Harvey, O. N. Jarvis, H. H. Duhm, J. Saudinos, and J. Mahoney, Phys. Lett. **26B**, 127 (1968).

[3]M. L. Barlett, J. H. McGill, L. Ray, M. M. Barlett, G. W. Hoffmann, N. M. Hintz, G. S. Kyle, M. A. Franey, and G. Blanpied, Phys. Rev. C **22**, 1168 (1980).

[4]R. J. Glauber, in *Lectures in Theoretical Physics,* edited by W. E. Brittin and L. G. Dunham (Interscience, New York, 1959), Vol. I, p. 315; in *High Energy Physics and Nuclear Structure, Proceedings of the Second International Conference, Rehovoth, 1967,* edited by G. Alexander (North-Holland, Amsterdam, 1967), p. 311; R. J. Glauber and G. Matthiae, Nucl. Phys. **B21**, 135 (1970).

[5]Y. Abgrall, J. Labarsouque, B. Morand, and E. Caurier, Nucl. Phys. **A316**, 389 (1979); J. Phys. G **6**, L55 (1980).

[6]J. N. Ginocchio, T. Otsuka, R. D. Amado, and D. A. Sparrow, Phys. Rev. C **33**, 247 (1986); G. Wenes, J. N. Ginocchio, A. E. L. Dieperink, and B. van der Cammen, Nucl. Phys. **A459**, 631 (1986).

[7]M. Abramowitz and I. A. Stegun, *Handbook of Mathematical Functions* (Dover, New York, 1965).

[8]A. Messiah, *Quantum Mechanics* (North-Holland, Amsterdam, 1961), Vol. II.